THERMOREGULATION

Self-sustaining personal all-day thermoregulatory clothing using only sunlight

Ziyuan Wang[1]†, Yiwen Bo[2]†, Peijia Bai[2], Shuchao Zhang[1], Guanghui Li[1], Xiangjian Wan[1], Yongsheng Liu[1]*, Rujun Ma[2]*, Yongsheng Chen[1]*

The human body must stay within a certain temperature range for comfort and safety. However, challenges for thermoregulatory clothing exist for harsh application scenarios, such as full day/night cycles, frigid polar regions, and space travel. We developed a flexible and sustainable personal thermoregulatory clothing system by integrating a flexible organic photovoltaic (OPV) module to directly acquire energy from sunlight and bidirectional electrocaloric (EC) devices. The flexible OPV-EC thermoregulatory clothing (OETC) can extend the human thermal comfort zone from 22°–28°C to 12.5°–37.6°C with a fast thermoregulation rate. The low energy consumption and high efficiency of the EC device allows for 24 hours of controllable and dual-mode thermoregulation with 12 hours of sunlight energy input. This self-powered wearable thermoregulatory platform has a simple structure, compact design, high efficiency, and strong self-adaptability with sunlight as the sole energy source.

Clothing plays an indispensable role in regulating body heat for preserving the thermal comfort of our body in daily life (*1*). One of the most common scenarios is to maintain body temperature within a safe range in situations of fluctuating and sometimes rapid changes in environmental temperature, for instance, walking from a comfortable indoor environment (~25°C) to a hot (>36°C) or cold (<15°C) outdoor environment. Without the ability to quickly adapt to such fast-changing environmental temperatures and cool down or warm up, people may become uncomfortable or sick and may even die (*2*). The more challenging scenarios are to keep our bodies in a comfortable temperature range (skin temperature) in harsh environments, such as frigid polar regions or space travel (which is extremely hot in sunlight but extremely cold in the dark). Therefore, wearable thermoregulatory clothing, capable of keeping the human body in a comfortable temperature range (skin temperature), as a spacesuit does, has been a long-sought but challenging goal for smart clothing systems.

Indeed, many thermoregulatory systems have been developed, which can be broadly classified into passive and active systems. Passive thermoregulatory systems include radiative thermoregulatory systems (*3*–*8*), phase-change thermoregulatory systems (*9*, *10*), and adsorption thermoregulatory systems (*11*, *12*). However, most systems powered by solar energy with self-sustainability can achieve only one-way thermoregulation (*3*–*5*, *8*). The systems that have bidirectional thermoregulation need to improve their efficiencies, response speeds and tunable temperature ranges (skin temperature) (*6*, *7*, *13*–*15*).

Active thermoregulatory systems allow for rapid cooling or warming of the human body. In general, cooling vests are based on coolant circulation or water/ice fluidic channels that allow for wearable thermoregulation; however, these systems require large and complex mechanical compressors (*16*, *17*). Although some excellent solid-state active thermoregulatory systems have been developed and the need for compressors and traditional liquid or vapor refrigerants could be eliminated, they still bear some substantial limits. For example, although the Joule effect heater is effective in heating with a controlled temperature, the high power consumption and lack of cooling capability strongly limit its application (*18*–*20*). The thermoregulatory systems based on magnetocaloric (*21*, *22*) and elastocaloric effects (*23*, *24*) require a large magnetic field and high mechanical load to realize good thermal-management effect, respectively, and thus have limited wearability. Thermoelectric (TE) thermoregulatory devices (*25*–*28*) based on the Peltier effect have found various applications. However, these devices generally exhibit low efficiency because of their high energy consumption. In particular, they all need extra energy input and cannot be kept working for a long period of time without additional energy. Although battery-based thermoregulatory systems can achieve good thermal-management performance in a short period of time, their limited energy supply cannot provide all-day and sustained thermoregulation for the human body (*25*, *27*).

Therefore, developing an all-day, self-powered, bidirectional thermoregulatory clothing system capable of rapidly responding to various complex or quick environmental temperature changes and keeping the human body in a comfortable temperature zone remains a challenging goal (*29*). The systems must harvest energy to achieve all-day thermoregulation. One of the more obvious sources of sustainable energy source is sunlight, which can be collected anywhere in open space. Indeed, solar cells, including an organic photovoltaic (OPV) cell, have evolved substantially (*30*), and the state-of-the-art OPV cell with a size of 4 mm^2 has a power conversion efficiency (PCE) of >20% (*31*). Simultaneously, flexible and high-performance OPV cells with PCEs >17% (*32*) have been demonstrated, which can be integrated into clothing to collect solar energy (*33*, *34*).

To achieve the required sustainability and flexibility as well as light weight, the thermal-management unit for the body must be highly efficient in transferring energy and have a low energy consumption. Therefore, we selected recently developed electrocaloric (EC) devices, which have high efficiency, low energy consumption, and bidirectional thermoregulatory properties and are pollution free (*35*–*38*). For example, one flexible EC thermoregulatory device has a very low energy cost, could reach a coefficient of performance of 13, and has a specific cooling power of 2.8 W/g (*35*).

We choose a flexible OPV module powered by sunlight and a high-efficiency heat transfer EC device as the two main units to fabricate a self-sustained thermoregulatory clothing system. We aim to power it only by solar energy with the capability of all-day (24 hours) cycling between hot/light and cold/dark environments. Our flexible OPV-EC thermoregulatory clothing (OETC) system exhibits highly efficient and fast performance in both cooling and warming modes as needed. Moreover, it can extend the thermal comfort zone by 19.1 K (from 6.0 to 25.1 K) and reach intelligent and controllable all-day dual-mode thermoregulation for the human body as needed. With the combination of these features, the human body wearing our OETC system can quickly adapt, as needed, to the changes of environmental temperature during outdoor activities and even possibly in such as harsh environments as polar regions or personal space travel.

Results and discussion

We fabricated a large flexible OPV module (*39*, *40*) with a thickness of only 180 μm for the sunlight energy–collecting unit in our OETC system (*41*). The entire flexible OPV module with an effective area of 25.2 cm^2 could provide a total voltage of 5.75 V and PCE of 11.85% under standard air mass 1.5 global (AM 1.5G, 100 mW/cm^2) (figs. S1 to S3 and table S1).

For the thermoregulatory unit in our OETC, we selected poly(vinylidene fluoride-trifluoroethylene-chlorofluoroethylene) [P(VDF-TrFE-CFE)], mainly because of its large entropy change, large

[1]State Key Laboratory and Institute of Elemento-Organic Chemistry, The Centre of Nanoscale Science and Technology and Key Laboratory of Functional Polymer Materials, Renewable Energy Conversion and Storage Center (RECAST), College of Chemistry, Nankai University, Tianjin 300071, China. [2]School of Materials Science and Engineering, National Institute for Advanced Materials, Nankai University, Tianjin 300350, China.
*Corresponding author. Email: yschen99@nankai.edu.cn (Y.C.), malab@nankai.edu.cn (R.M.), liuys@nankai.edu.cn (Y.L.)
†These authors contributed equally to this work.

adiabatic temperature change near room temperature, and good mechanical flexibility (*42*). The EC system based on P(VDF-TrFE-CFE) has substantial potential for efficient thermoregulation (*35*, *36*, *43*). We fabricated a flexible EC thermoregulatory device following Ma *et al.* (*35*, *44*) (fig. S4). Noticeably, our flexible EC device exhibits the same thermal-management performance as the rigid one (figs. S5 and S6).

With these two flexible units ready, we integrated them together for the OETC system (fig. S7). In sunlight, the OPV module efficiently converts solar energy into electrical energy to drive the EC device directly to provide a cooling effect (Fig. 1). The excess energy can be stored in a simple attached energy storage system (ESS) (fig. S8) because of the low energy consumption of the EC device, as discussed below. The power provided by the OPV is sufficient to power the entire OETC system (see fig. S8 for details). Therefore, in the dark, our OETC system can use the stored energy provided by the ESS to maintain body temperature when the environment is cold and thus achieve a full day (day/night) of operation. The cooling mode and warming mode can be switched as desired at any time to achieve individual thermal comfort.

Working mechanism of the OETC system in cooling/warming mode

We show a photograph of the flexible OETC thermoregulation system assembled by one OPV module and two EC units (Fig. 2A). This compact assembly mode can provide effective cooling/warming for the human body as needed. The working mechanism of the OETC system for the cooling mode (Fig. 2B) is the same as that powered by the electric supply (*37*), but in our system, we power it directly by the electricity generated by the OPV module (see fig. S9 for details). The cooling mode includes the following steps (*35*): (i) electrostatic actuation of the EC polymer stack toward the top flexible heat transfer layer (as a heat sink with large heat capacity) (fig. S10); (ii) the EC polymer stack is heated up by applying an electric field on the EC polymer stack, and thus, heat transfers from the EC polymer stack to the flexible heat transfer layer [Fig. 2B, (1)]; (iii) electrostatic actuation of the EC polymer stack toward the bottom human skin (as a heat source); (iv) the EC polymer stack is cooled down by removing the electric field, and thus, heat transfers from the human skin to the EC polymer stack to realize one cycle of skin cooling [Fig. 2B, (2)]. For the warming mode, warming is achieved by changing the heat transfer to the opposite direction by changing the sequence of the four steps described above, which is realized by simply adjusting the phase of square-wave voltage. Correspondingly, the warming mode has similar steps to the cooling mode but with the opposite heat transfer effect: (i) electrostatic actuation of the EC polymer stack toward the bottom human skin that needs to be warmed up; (ii) the EC polymer stack is heated up by applying an electric field on the EC polymer stack, and thus, heat transfers from the EC polymer stack to the human skin (as a heat sink) [Fig. 2B, (3)]; (iii) electrostatic actuation of the EC polymer stack toward the top flexible heat transfer layer (as a heat source); (iv) the EC polymer stack is cooled down by removing the electric field, and thus, heat transfers from the flexible heat transfer layer to the EC polymer stack to finish one cycle of skin warming [Fig. 2B, (4)]. With these two working modes, bidirectional controllable thermoregulation for cooling and warming can be implemented as needed.

Electrostatic actuation is a simple and fast method to control the heat transport speed by adjusting the working frequency of the EC device (*35*–*37*, *43*). We compared the temperature span of the OETC system at different frequencies under the standard AM 1.5G (100 mW/cm^2) by a solar simulator (fig. S11). Although the OETC system can operate at higher frequencies, the frequency of the OETC system that gives a maximum temperature span of 2.9 K is 0.75 Hz (one complete cycle takes ~1.33 s), in part because of the time needed to transfer the heat from EC stack to human skin and flexible heat transfer layer.

Temperature span of the OETC system in different working scenarios

The temperature span of our OETC thermoregulation can also be easily adjusted by the illumination intensity. With the increase of illumination intensity, the flexible OPV module can reach higher voltage (power), and thus, the input voltage of the EC device increases (fig. S12), which results in a higher thermoregulatory performance of the OETC system. We measured the temperature difference (ΔT, difference between real-time temperature and initial temperature) of the OETC system under different illumination intensities of 55 (fig. S13), 70, and 100 mW/cm^2 irradiation using a solar simulator at a frequency of 0.75 Hz (Fig. 2C). The OETC system works well at different illumination intensities, and the maximum temperature span can reach 2.9 K when the illumination intensity is standard AM 1.5G sunlight (100 mW/cm^2). Furthermore, the outdoor thermoregulation performance of our OETC system was also demonstrated by direct solar radiation under clear sky conditions from 9:00 to 16:00 in Tianjin, China (3 August 2022) (fig. S14). Although the intensity of outdoor sunlight varies considerably with time, our OETC system still shows good and stable thermal-management ability at different illumination intensities. When the outdoor sunlight intensity is the same as the simulated illumination intensity, the OETC system exhibits almost the same thermal management (Fig. 2C and fig. S14B). The whole process runs without external energy sources and realizes self-powered thermoregulation with zero energy consumption.

Although an outside electric supply was previously required to power the EC device to achieve the effective thermal management reported in the literature (*35*–*37*, *43*), we demonstrated that the EC device can instead be powered directly on site by an integrated flexible OPV module. The integrated device shows the same outstanding performance, including the same temperature difference (ΔT) at the same electric field (Fig. 2D).

Excellent sustainable performance of the OETC system

We compared the thermoregulatory performance of the commercial rigid TE device of the same size as the EC device powered by a

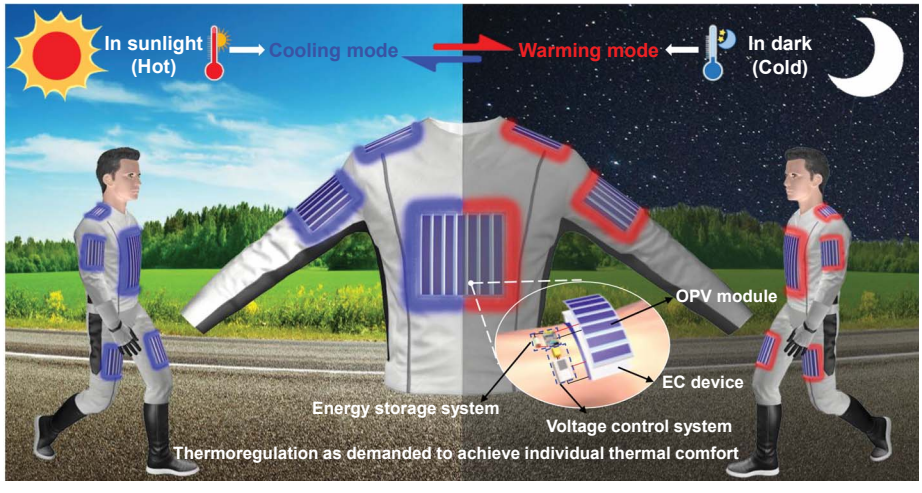

Fig. 1. Working schema when wearing our flexible OETC to achieve individual thermal comfort in a cycle between hot (in sunlight) and cold (in dark) environments as demanded.

flexible OPV module under an illumination intensity of 100 mW/cm^2 (Fig. 2E and fig. S15). The temperature span (Fig. 2E) and heat flux (figs. S15C and S16) of our OETC system are 2.9 K and 28.76 mW/cm^2, respectively, whereas the OPV-TE system shows only the temperature span of 1.2 K (Fig. 2E and fig. S15B) and heat flux of 16.79 mW/cm^2 (fig. S15C), respectively, under the same illumination intensity of 100 mW/cm^2. In addition, we also compared the thermoregulatory performance of the perovskite photovoltaic module with a similar size to that of the EC device powered by an OPV module under the illumination intensity of 100 mW/cm^2 (fig. S17). Compared with the thermal-management performance of the EC device powered by OPV module in Fig. 2C, the EC device powered by the perovskite solar module (fig. S17) displayed almost same results. Meanwhile, we calculated the power consumption of the EC device under different illumination intensities (fig. S18). Under the illumination intensity of 100 mW/cm^2, the average power consumption of the EC device is only 1.91 mW/cm^2 at 0.75 Hz because of its low energy consumption. Considering that the PCE of our OPV module (with an active area of 25.2 cm^2) is 11.85% under standard AM 1.5G (100 mW/cm^2) and the energy consumption of the EC device (with an active area of 8 cm^2) is only 15.28 mW (1.91 mW/cm^2 × 8 cm^2 = 15.28 mW), a simple estimate indicates that the total generated electricity is 298.58 mW (100 mW/cm^2 × 11.85% × 25.2 cm^2 = 298.58 mW). Thus, we benefit from the low energy consumption (15.28 mW) of the EC device, with 283.30 mW (298.58 mW − 15.28 mW = 283.30 mW) of surplus energy that could be stored under ideal conditions (figs. S8 and S19). The surplus energy stored in the ESS could be automatically switched to power the entire system at night with no extra energy input to realize a full day/night thermoregulatory cycle (fig. S20). Moreover, it is worthwhile to note that energy recovery is also possible during the depolarization process of the EC effect (*43*), which thus further improves the efficiency of our OETC system.

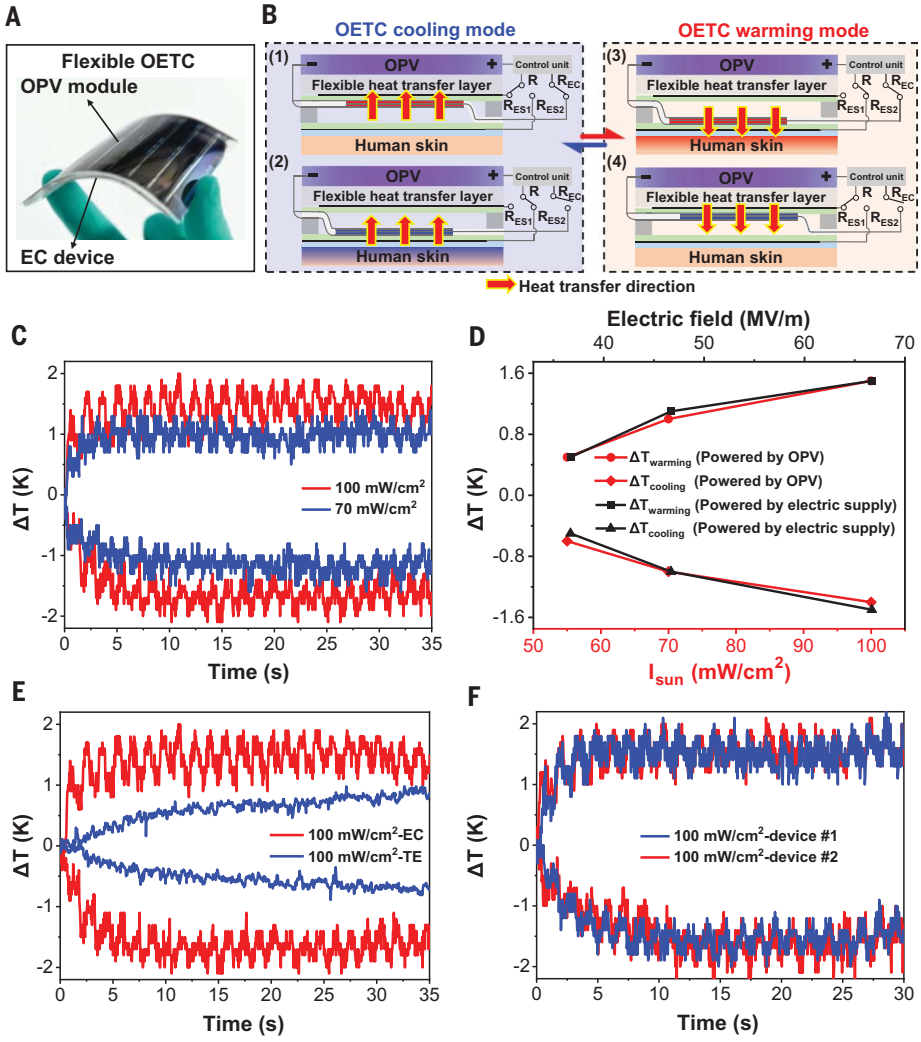

Fig. 2. Performance of the flexible OETC system. (**A**) Photograph of an OETC system assembled by an OPV module and two EC units. (**B**) Working mechanism of the OETC system in cooling/warming mode, respectively. The cooling/warming mode can be easily switched by the control unit when moving from a thermal comfort environment into a hot/cold environment. R_{ES}, the relay for controlling the electrostatic actuation. (**C**) Temperature span of the OETC system under different illumination intensities (70 and 100 mW/cm^2) in cooling/warming mode at 0.75 Hz. (**D**) Comparison of ΔT of the EC thermoregulation device driven by OPV module and electric supply under different electric fields. (**E**) Comparison of temperature span of EC and TE thermoregulation devices with the same size (active area of 8 cm^2) driven by the same OPV module under an illumination intensity of 100 mW/cm^2. (**F**) Temperature span of two EC parallel array devices (active area of 16 cm^2) driven simultaneously by one OPV module (active area of 25.2 cm^2) under an illumination intensity of 100 mW/cm^2.

Performance of an OPV-EC array

The EC devices have good array cooperativity, and one single OPV module with an active area of 25.2 cm^2 has sufficient power to simultaneously drive two parallel arrays of EC devices with an active area of 16 cm^2. For example, under standard AM 1.5G (100 mW/cm^2), the two EC parallel devices could be synchronized completely, and both could reach a temperature span of 2.9 K, which demonstrates their bidirectional thermoregulatory performance (Fig. 2F). To further extend its application in wearable thermoregulation, we evaluated the performance of four parallel EC arrays driven by one OPV module under an illumination intensity of 100 mW/cm^2 (fig. S21). Four parallel EC arrays can simultaneously achieve bidirectional controllable thermoregulation (movie S1). This indicates that our OETC system has good scalability required for the practical wearable thermoregulation.

Thermoregulatory performance of OETC on the human body

To demonstrate the wearability of the OETC for meeting the flexible needs of human body thermoregulation, we measured the stability of OETC cooling and warming mode performance in the bending state (Fig. 3A and fig. S22). During the bending measurement, the system is illuminated with a 100 mW/cm^2 light at the bottom, and the surface temperature is measured by an infrared camera at the top (movie S2). Our OETC reaches its maximum and stable thermoregulation performance when it starts to operate at 0.75 Hz for 10 s. The initial state of the OETC is flat, and the radius of curvature (k) of OETC is 0 m^{-1}. Then, the OETC system is bent at a uniform rate of 0.12 m^{-1} s^{-1} to reach a maximum curvature of 3.6 m^{-1}, followed by the same rate of bending release until the curvature of the OETC returns to 0 m^{-1}. During the operation, we observed negligible change in its thermoregulatory performance in the flat, bent, and released states of the OETC, which demonstrates excellent flexibility.

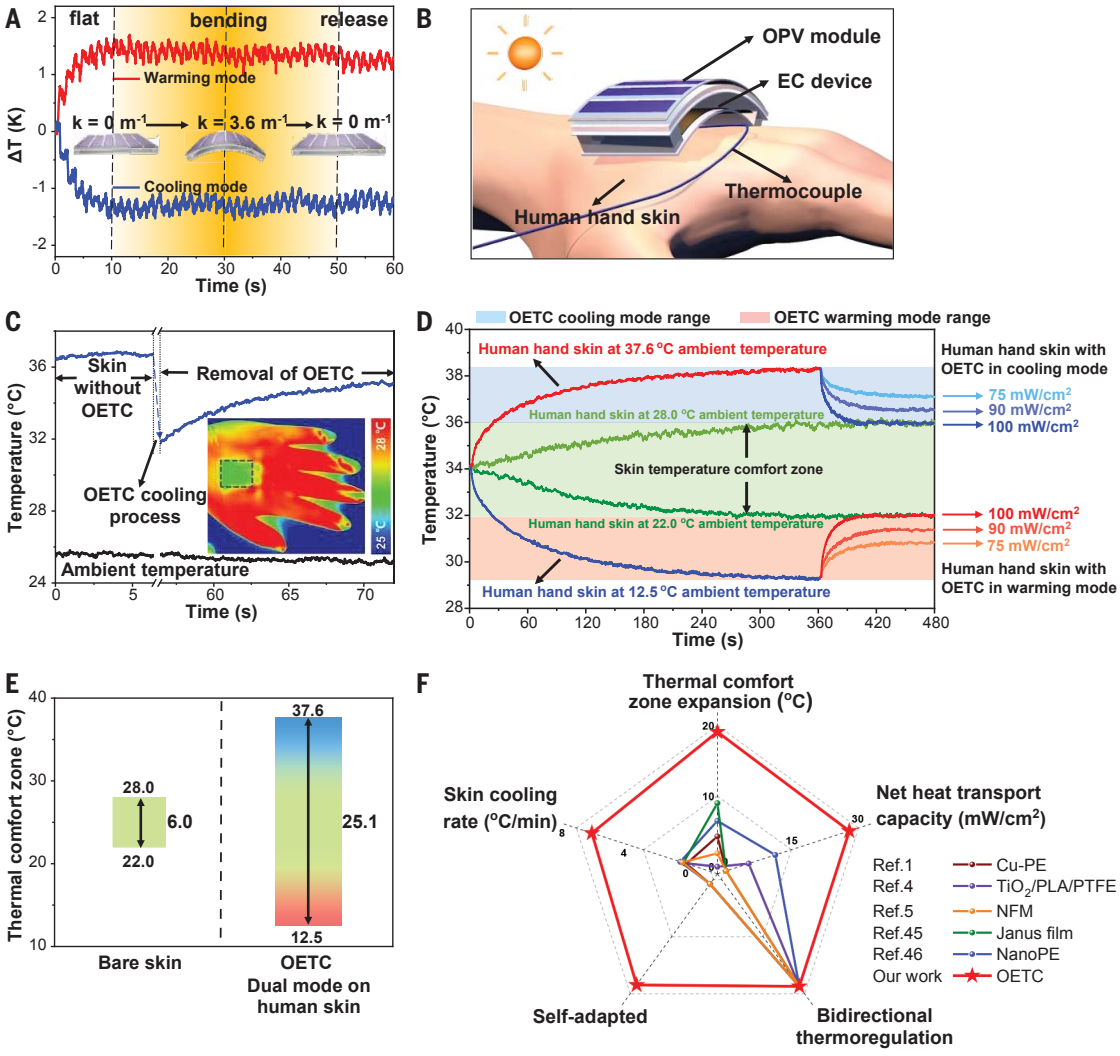

Fig. 3. Wearable thermoregulatory performance of OETC. (**A**) Performance of the flexible OETC under different curvature. (**B**) Schematic of the thermoregulatory setup consists of the skin, a thermocouple measuring the temperature of the skin, and OETC covering the skin. (**C**) Thermoregulation of human hand in OETC cooling mode. The inset is the infrared thermal image of a human hand in OETC cooling mode. (**D**) Thermoregulation of the human hand skin by OETC under different sunlight intensity (75, 90, 100 mW/cm^2) at different environmental temperatures. The initial temperature of the skin is 34.0°C. When moving the skin into different environmental temperatures of 37.6° and 12.5°C, the skin can reach 38.3° and 29.2°C, respectively. By using the OETC cooling mode at high environmental temperature and warming mode at low temperature under standard AM 1.5G (100 mW/cm^2), the human skin temperature can be maintained in the thermal comfort temperature range of 32.0° to 36.0°C (skin temperature), even though the environmental temperature changes between 12.5° and 37.6°C. When the illumination intensity is lower than 100 mW/cm^2 (75 or 90 mW/cm^2), our OETC system still has bidirectional thermoregulation performance. (**E**) Thermal comfort zone of bare human skin and human skin with OETC dual working mode. (**F**) Comparison of the net power, thermal comfort zone expansion, cooling capability for skin, bidirectional thermoregulation, and self-adaptability of the OETC with related representative works reported in the literature (*1*, *4*, *5*, *45*, *46*). The definitions of Cu-PE, TiO_2/PLA/PTFE, NFM, Janus film, and NanoPE are given in the supplementary text.

We further applied the flexible OETC to human skin for thermoregulation. We show the experimental setup of the flexible OETC thermal measurement on the human skin (Fig. 3B) and the thermoregulation of a human hand in OETC cooling mode (Fig. 3C). We monitored the whole process with an infrared camera detector under an illumination intensity of 100 mW/cm^2 at an environmental temperature of 26°C. Our OETC cooled the human skin from 36.8° to 31.7°C at an average rate of 6.1°C/min to achieve fast thermoregulation (Fig. 3C).

The human body must remain within a certain temperature range (skin temperature) for a comfortable and safe existence, but this range varies individually (*45*–*47*). We set a comfort range on the basis of observed human skin temperatures between 32° and 36°C (*46*), which requires an environmental temperature range between 22° and 28°C (thus, the thermal comfort zone of bare human skin is 6.0 K in our measurement) (Fig. 3D).

We measured the thermoregulation performance on human skin directly, with the human hand temperature starting at 34.0°C and a corresponding environmental temperature of 25.0°C (the middle point of the comfort zone). Under standard AM 1.5G (100 mW/cm^2), when moving the skin into a low-temperature environment (12.5°C), the skin temperature drops to 29.2°C and the OETC warming mode starts working, which raises the skin temperature up to the thermal comfort temperature of 32.0°C (Fig. 3D). Correspondingly, when moving the skin into a higher-temperature environment of 37.6°C, the skin temperature rises to 38.3°C. The OETC cooling mode turns on, which brings the skin temperature down to the thermal comfort temperature of 36.0°C.

As a result, our OETC maintains human skin temperature within a thermal comfort zone between 32.0°C and 36.0°C, even though the environmental temperature varies between 12.5° and 37.6°C. Compared with bare human skin (thermal comfort zone of 6 K), our OETC extends the thermal comfort zone of the skin by 19.1 K (Fig. 3E) for this module size and illumination intensity. In addition, skin can be warmed at a maximum rate of 15.6°C/min or cooled at a maximum rate of 14.0°C/min in the first 5 s to achieve fast thermoregulation. When the illumination intensity is lower than 100 mW/cm^2 (75 or 90 mW/cm^2), our OETC system still has bidirectional thermoregulation performance. Under an illumination intensity of 90 mW/cm^2, the OETC warming

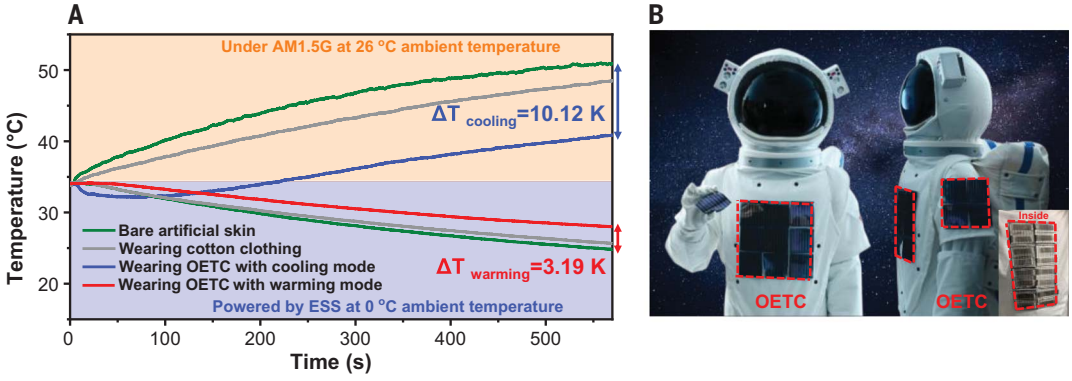

Fig. 4. The thermoregulation performance of OETC compared with cotton clothing and prospect of personal space travel. (**A**) Temperature changes of bare artificial skin, skin wearing cotton clothing, and skin wearing OETC in the sunlight of 100 mW/cm^2 at a 26°C environment temperature and in the dark at a 0°C environment temperature, respectively. The initial temperature of the artificial skin is 34°C, and the temperature is measured by thermocouples. (**B**) Photograph of the OETC worn on the human body for the prospect of personal space travel.

mode can raise the skin temperature from 29.4° to 31.3°C, whereas the OETC cooling mode could lower the skin temperature from 38.3° to 36.5°C. These temperatures fall only slightly outside the thermal comfort zone. When the illumination intensity is 75 mW/cm^2, the OETC system still can bidirectionally thermoregulate the skin from 29.4° to 30.8°C in warming mode and from 38.3° to 37.2°C in cooling mode. Furthermore, we also evaluate the thermoregulation performance of OETC on artificial skin at 100 mW/cm^2 under different environmental temperatures (fig. S23). The thermal comfort zone of bare artificial skin is from 23° to 27°C (4.0 K) (*46*); OETC extends the thermal comfort zone of the artificial skin by 16.6 K (fig. S23A). Although OETC cannot restore the temperature of artificial skin to the thermal comfort zone in a harsher environment, it still has good thermoregulation performance (fig. S23B). Improvements in the thermal comfort zone can be made with performance or efficiency improvements in the OPV or EC units. Alternatively, the relative ratios and sizes of the OPV and EC units could be further optimized.

We summarize the net heat transport capacity, thermal comfort zone expansion, skin cooling rate, bidirectional thermoregulation, and self-adaptability of our OETC compared with related representative works reported in the literature (Fig. 3F) (*1*, *4*, *5*, *45*, *46*). By benefiting from the efficient net heat transport capacity of 27.89 mW/cm^2 (fig. S16), our OETC can extend the human thermal comfort zone by 19.1 K. Moreover, the OETC system can effectively cool the human skin at an average rate of 6.1°C/min to achieve fast thermoregulation. By benefiting from the low energy consumption of the EC device, the OETC system could operate a full 24 hours with 12 hours of sunlight energy input (fig. S18). Thus, the combined characteristics of our personal thermoregution system, such as controllable, all-day dual mode and notable thermoregulation performance, could make it possible for individuals to stay more comfortable in harsh environments while using only sunlight as the energy source.

Thermoregulation performance of OETC in the outdoors and the prospect for use in space

We measured and compared the temperature changes of bare artificial skin, skin covered with cotton clothing, and skin covered with an OETC (Fig. 4A) in sunlight of 100 mW/cm^2 at 26.0°C environmental temperature and in the dark at 0°C environmental temperature, respectively. Under an illumination intensity of standard AM 1.5G (100 mW/cm^2) at 26.0°C environmental temperature, the temperature of bare skin and skin covered with cotton clothing can be raised from 34.0°C up to 50.9° and 48.4°C, respectively. Nevertheless, the temperature of the artificial skin covered with an OETC is only 40.8°C. The maximum cooling capacity reaches 10.1 K (calculated by the temperature difference between bare artificial skin and artificial skin covered with an OETC in cooling mode after 570 s exposed to an illumination intensity of 100 mW/cm^2 in a 26.0°C environmental temperature), which demonstrates the cooling power of OETC. In addition, OETC can be driven to warm the skin by using the ESS in cold night at a 0°C environmental temperature. The warming performance of artificial skin covered with an OETC compared with artificial skin is 3.2 K (calculated by the temperature difference between bare artificial skin and artificial skin covered with an OETC in warming mode after 570 s exposed to the 0°C environmental temperature) higher than those of skin covered with cotton clothing and bare skin, which demonstrates the excellent warming capacity of OETC.

The bidirectional thermoregulation that uses solar power could make this device of interest for integrating into a conventional spacesuit to help reduce the overall power requirements (Fig. 4B). During individual space travel, the theoretical area of a spacesuit is around 1.85 m^2 (*48*). In space, the magnitude of the solar radiation pressure depends on the solar flux near the surface of Earth, and a solar constant of 136.7 mW/cm^2 is normally used to calculate the solar flux in 1 astronomical unit (*49*). With continued improvements in solar cell performance, including that of the flexible OPV module, if we assume that a 45% PCE solar cell device is used, we estimate that an OPV module to provide all-day human body thermoregulation will have an area of only 1.12 m^2 (*50*). We believe that this OETC system could be optimized in the future in terms of both performance and practicability for application in harsher environments. The temperature span of the EC device can be increased to improve the thermoregulation performance of our OETC system. First, for the material side, the double bond–modified P(VDF-TrFE-CFE) materials could provide a larger temperature change of 7.8 K at 118 MV/m (*37*). Second, the device could be optimized by using a cascade device to increase the temperature span of 4.8 K (double-deck) and 8.7 K (four-layer cascade) (*38*, *45*). Lastly, by adding nanofillers to improve the thermal conductivity of P(VDF-TrFE-CFE) (*51*) or by using an active EC regenerator to further increase the temperature span (*52*, *53*), the EC performance can be further improved. Clearly, further studies are needed to develop a practical product based on the prototype and concept demonstrated in this work.

Conclusions

We developed an advanced self-powered wearable thermoregulatory system that integrates flexible OPV module and EC thermoregulation units together for efficient personalized thermoregulation. Its active control feature can be used for fast cooling/warming dual-mode thermoregulation as needed by the human body. Moreover, the thermal comfort zone can be extended from 6.0 to 25.1 K by OETC with rapid thermoregulation, which can ensure the safety and comfort of the human body in various complex and unstable environments. By benefiting from the low energy consumption of the EC device, OETC can achieve controllable and all-day dual-mode thermoregulation. Together with its other outstanding features such as simple and compact structure, high efficiency, and strong self-adaptability, with more optimization, we believe that the OETC could

demonstrate potential applications in the field of high-end thermoregulation and even extend human survivability in harsh environments such as polar regions and individual space walking.

REFERENCES AND NOTES

1. J. Chai *et al*., *Cell Rep. Phys. Sci.* **3**, 100958 (2022).
2. ANSI/ASHRAE, *Standard 55: Thermal Environmental Conditions for Human Occupancy* (American Society of Heating, Refrigerating, and Air-Conditioning Engineers, 2017).
3. X. A. Zhang *et al*., *Science* **363**, 619–623 (2019).
4. S. Zeng *et al*., *Science* **373**, 692–696 (2021).
5. R. Xiao *et al*., *ACS Appl. Mater. Interfaces* **11**, 44673–44681 (2019).
6. Q. Zhang *et al*., *Nat. Commun.* **13**, 4874 (2022).
7. Q. Zhang, Y. Wang, Y. Lv, S. Yu, R. Ma, *Proc. Natl. Acad. Sci. U.S.A.* **119**, e2207353119 (2022).
8. P.-C. Hsu *et al*., *Science* **353**, 1019–1023 (2016).
9. Y. Kou *et al*., *Energy Storage Mater.* **34**, 508–514 (2021).
10. Z. Luo *et al*., *Adv. Funct. Mater.* **33**, 2212032 (2023).
11. C. Wang *et al*., *Joule* **4**, 435–447 (2020).
12. J. A. Mason *et al*., *Nature* **527**, 357–361 (2015).
13. L. Zhou *et al*., *Cell Rep. Phys. Sci.* **2**, 100338 (2021).
14. H. Luo *et al*., *Nano Lett.* **21**, 3879–3886 (2021).
15. L. Zhang *et al*., *Angew. Chem. Int. Ed.* **54**, 3952–3956 (2015).
16. M. Mokhtari Yazdi, M. Sheikhzadeh, *J. Text. Inst.* **105**, 1231–1250 (2014).
17. M. Smith, V. Cacucciolo, H. Shea, *Science* **379**, 1327–1332 (2023).
18. G.-X. Li, T. Dong, L. Zhu, T. Cui, S. Chen, *Chem. Eng. J.* **453**, 139763 (2023).
19. Y. Guo *et al*., *Small* **13**, 1702645 (2017).
20. Z. Guo, C. Sun, J. Wang, Z. Cai, F. Ge, *ACS Appl. Mater. Interfaces* **13**, 8851–8862 (2021).
21. D. J. Silva, B. D. Bordalo, A. M. Pereira, J. Ventura, J. P. Araújo, *Appl. Energy* **93**, 570–574 (2012).
22. Y. Liu *et al*., *Nat. Commun.* **7**, 11614 (2016).
23. S. Zhang *et al*., *Nat. Commun.* **13**, 9 (2022).
24. R. Wang *et al*., *Science* **366**, 216–221 (2019).
25. J. Choi, C. Dun, C. Forsythe, M. P. Gordon, J. J. Urban, *J. Mater. Chem. A Mater. Energy Sustain.* **9**, 15696–15703 (2021).
26. H. Wei, J. Zhang, Y. Han, D. Xu, *Appl. Energy* **326**, 119941 (2022).
27. Y. Zhang *et al*., *ACS Appl. Mater. Interfaces* **14**, 15317–15323 (2022).
28. R. A. Kishore, A. Nozariasbmarz, B. Poudel, M. Sanghadasa, S. Priya, *Nat. Commun.* **10**, 1765 (2019).
29. R. Mutschler, M. Rüdisüli, P. Heer, S. Eggimann, *Appl. Energy* **288**, 116636 (2021).
30. L. Meng *et al*., *Science* **361**, 1094–1098 (2018).
31. J. Wang *et al*., *Natl. Sci. Rev.* **10**, nwad085 (2023).
32. G. Zeng *et al*., *J. Am. Chem. Soc.* **144**, 8658–8668 (2022).
33. H. Jinno *et al*., *Nat. Energy* **2**, 780–785 (2017).
34. A. Sharma *et al*., *Appl. Mater. Today* **29**, 101614 (2022).
35. R. Ma *et al*., *Science* **357**, 1130–1134 (2017).
36. Y. Bo *et al*., *Adv. Energy Mater.* **11**, 2003771 (2021).
37. P. Bai *et al*., *Adv. Mater.* **35**, e2209181 (2023).
38. H. Cui *et al*., *Joule* **6**, 258–268 (2022).
39. C.-Y. Liao *et al*., *Joule* **4**, 189–206 (2020).
40. S. Zhang *et al*., *Sol. RRL* **7**, 2300029 (2023).
41. See "Preparation of the flexible large-area OPV module" in the materials and methods for the detailed procedure.
42. B. Neese *et al*., *Science* **321**, 821–823 (2008).
43. Y. Meng *et al*., *Nat. Energy* **5**, 996–1002 (2020).
44. See "Preparation of the flexible EC device" in the materials and methods for the detailed procedure.
45. B. Dai, X. Li, T. Xu, X. Zhang, *ACS Appl. Mater. Interfaces* **14**, 18877–18883 (2022).
46. P.-C. Hsu *et al*., *Sci. Adv.* **3**, e1700895 (2017).
47. F. Salata, I. Golasi, V. Ciancio, F. Rosso, *Build. Environ.* **146**, 50–63 (2018).
48. J. G. Metts, J. A. Nabity, D. M. Klaus, *Adv. Space Res.* **47**, 1256–1264 (2011).
49. O. Montenbruck, P. Steigenberger, U. Hugentobler, *J. Geod.* **89**, 283–297 (2014).
50. See "Calculation of the required OPV module area to provide all-day thermoregulation for individual space travel" in the supplementary text for details.
51. G. Zhang *et al*., *Adv. Mater.* **27**, 1450–1454 (2015).
52. A. Torelló *et al*., *Science* **370**, 125–129 (2020).
53. Y. Wang *et al*., *Science* **370**, 129–133 (2020).

ACKNOWLEDGMENTS

We gratefully acknowledge the financial support from the National Key R&D Program of China (2022YFB4200400, 2019YFA0705900, 2020YFA0711500), the National Natural Science Fund of China (21935007, 52025033, 51973095, and 52273248), and the Key Project of Natural Science Foundation of Tianjin City (21JCZDJC00010). **Funding:** National Key R&D Program of China (2022YFB4200400, 2019YFA0705900, 2020YFA0711500); National Natural Science Fund of China (21935007, 52025033, 51973095, and 52273248); and Key Project of Natural Science Foundation of Tianjin City (21JCZDJC00010). **Author contributions:** Y.C. and R.M. conceived and designed the project. Z.W. and Y.B. fabricated the OETC thermoregulation system and carried out the OETC performance studies. S.Z. and Z.W. fabricated the OPV module. Y.B. and P.B. fabricated the EC thermoregulation system. Z.W., Y.B., G.L., X.W., Y.L., R.M., and Y.C. analyzed and interpreted the data. The manuscript was mainly prepared by Y.C., R.M., Z.W., and Y.B. All authors reviewed and commented on the manuscript. **Competing interests:** Y.C., R.M., Y.L., Z.W., Y.B., and Y.Z. are inventors on a China provisional patent application serial number 2023110782432, related to this work. The authors declare no competing interests. **Data and materials availability:** All data are available in the main text or the supplementary materials.

SUPPLEMENTARY MATERIALS

science.org/doi/10.1126/science.adj3654
Materials and Methods
Supplementary Text
Figs. S1 to S23
Table S1
References (*54*–*59*)
Movies S1 and S2

Submitted 23 June 2023; accepted 24 October 2023
10.1126/science.adj3654

Self-sustaining personal all-day thermoregulatory clothing using only sunlight

Ziyuan Wang, Yiwen Bo, Peijia Bai, Shuchao Zhang, Guanghui Li, Xiangjian Wan, Yongsheng Liu, Rujun Ma, and Yongsheng Chen

Science **382** (6676), . DOI: 10.1126/science.adj3654

Editor's summary

Clothing often helps to regulate comfort, but it is normally focused on keeping a person either warmer or cooler. Wang *et al*. developed a thermoregulatory clothing system that combines an organic photovoltaic with bidirectional electrocaloric devices that are capable of heating or cooling (see the Perspective by Huang and Li). Both components are flexible, which is important for personal thermal regulation applications. The device runs off of sunlight, so no additional power sources are needed, and it could be useful in a variety of harsh environments. —Brent Grocholski